# Numerical study of strength mismatch in cross-weld tensile testing

## Conference or Workshop Item

*International Congress on **A**dvances in **W**elding **S**cience and **T**echnology for Construction, Energy and Transportation Systems (AWST - 2011)*
*24-25 October 2011, Antalya, Turkey*

AWST-11/87

# Numerical Study of Strength Mismatch in Cross-Weld Tensile Testing

**M. O. Acar[1,a], S. Gungor[1,b], M. E. Fitzpatrick[1,c], P. J. Bouchard[1,d]**

[1] Materials Engineering, The Open University, Walton Hall, Milton Keynes MK7 6AA, UK

[a]m.o.acar@open.ac.uk, [b]s.gungor@open.ac.uk, , [c]m.e.fitzpatrick@open.ac.uk, [d]p.j.bouchard@open.ac.uk

## Abstract

The strength mismatch effect on the deformation behaviour of defect-free cross-weld tensile specimens, where there is a variation in strength along the length of the specimen, was investigated through 2D finite element analysis. A simple bi-material model, which is generally used in current engineering assessments (e.g. R6 "Assessment of the integrity of structures containing defects") to examine the strength mismatch effect on the deformation and fracture behaviour of a weld which actually includes a heat-affected-zone, could lead to non-conservative or overly conservative predictions. In fusion welded components, one would generally observe that there is a heat-affected zone where the material properties are different from the weld and base material, and there is a continuous gradient of properties between the two. The material properties in HAZ are generally assigned discretely; however, in our multi-material model these properties are successfully assigned continuously by embedding subroutines into finite element model. This multi-material approach was used to examine the effect of strength mismatch on the local and global deformation behavior of fusion welds. It has been found that the bi-material modeling, by ignoring the HAZ, and multi-material discrete HAZ modeling of the cross-weld specimens leads to unrealistically biaxial stresses at the interfaces where there is an abrupt variation of the material properties. However, multi-material continuous HAZ modeling eliminates unrealistic stress biaxiality and enables to examine the local deformation more accurately. It was also found that the global stress-strain behaviour obtained using the bi-material and multi-material modeling is different.

***Keywords:*** *Cross-weld, Tensile testing, Finite Element Analysis*

## 1. Introduction

The structural integrity, performance and life of austenitic stainless steel weldments in power generation plants are determined by the mechanical properties of the weld metal, the heat affected zone (HAZ) and the base metal. Tube junctions in heat exchanger units are often produced by tube-shaping (e.g. bending, swaging) and fusion welding. Therefore, it is likely that welding is performed onto the base metal which was hardened during tube-shaping. Although the standard codes and construction practices [1, 2] bring some limitations to put these as-produced components into service, it is sometimes not possible to follow these rules strictly especially when the whole boiler was constructed as a single unit which was then too large and too complex and contained different tubing materials [3]. Therefore, some weldments in service consist of a strain-hardened base metal, a considerable range of heat affected zone and the weld metal.

In a project investigating the HAZ cracking in tube junctions, the local mechanical properties were determined spatially on flat cross-weld specimens which have different strength mismatch levels by conducting digital image correlation integrated tension tests. For better understanding and validation of the experimental results reported in [4], the tension tests of cross-weld specimens were simulated in ABAQUS. In this paper, the numerical results obtained through three different finite element models in which the material properties of the HAZ are assigned in different ways will be discussed to understand the influence of the strength mismatch and HAZ material modelling on local and global deformation behavior.

## 2. Finite Element Analysis

The geometry of the flat cross-weld specimens used in the bi-material and multi-material models and the boundary conditions are presented in Figure 1. The specimens are 70mm in length with a gauge length of 63.3mm and 8mm (height) × 6mm (width) weld in the middle. 2D plane stress condition was imposed. Quadrilateral CPS8R (reduced integration, eight-node element) type plane stress elements were used. The boundary conditions are selected as in the actual tension tests of cross-weld specimens; the bottom end of the specimen is fixed and a constant displacement rate of 0.1mm/min is applied in *y*-direction from the top end. All FE analyses in this study are non-linear and based on

isotropic elastic–plastic materials with isotropic work-hardening.

The strength mismatch level in cross-weld specimens can be described as the ratio between the yield strength of the weld metal and the base metal. It is defined by

$$M = \frac{\sigma_y^{weld}}{\sigma_y^{base}} \quad (1)$$

M<1 refers to under-matched condition and M>1 refers to over-matched condition. Two under-matched conditions with strength mismatch level of 0.6 and 0.42 were considered in this study.

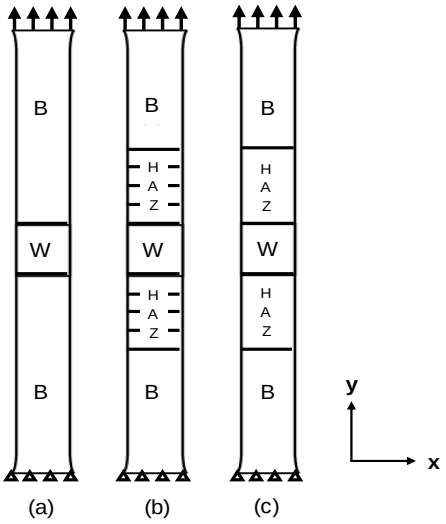


**Figure 1. The geometry of the cross-weld tensile specimens and the boundary conditions for bi-material (a), and multi-material models with discrete HAZ (b) and continuous HAZ (c) (B: Base metal and W: Weld metal)**

### 2.1. Bi-material model

The bi-material model consists of a soft weld and a strong base metal, but the HAZ is neglected, as shown in Figure 1(a). The variation of the yield strength along the length of the specimen is given for two different mismatch levels in Table 1. Note that the material properties abruptly changes at the weld/parent interface. Stress singularity could occur at the interface due to the strength mismatch; therefore, a fine mesh size (0.1mm) was used around the interface.

### 2.2. Multi-material models

In fusion welds, the heat flow from the molten weld towards the base metal alters the material properties of the base metal. For example, in multi-pass welds, the base metal near the fusion boundary may undergo cyclic strain hardening due to the thermal cycles during welding [5]. Another example is the softening of the base metal that was cold-worked prior to welding [6]. In both cases, there is a heat affected region where the material properties are different from the base metal and the weld metal and hence there is a continuous gradient of material properties in between two.

In FE simulations, the material properties in HAZ are commonly defined discretely by assigning intermediate material properties into discrete HAZ layers [7-9] or as a single HAZ material [10, 11]. In our multi-material discrete HAZ model, HAZ was divided into four layers as shown in Figure 1(b) and intermediate material properties were assigned into those layers. The yield strength variation along the length of the specimen is given for multi-material discrete HAZ model in Table 1. A fine mesh size was used as in the bi-material model due to the stress singularity problem at the interfaces between different HAZ layers and the weld/HAZ1 interface.

**Table 1 The variation of the 0.002 offset yield strength along the length of the under-matched cross-weld specimens with strength mismatch level of M=0.6 and M=0.42**

| | | Base metal | HAZ4 | HAZ3 | HAZ2 | HAZ1 | Weld metal |
|---|---|---|---|---|---|---|---|
| M=0.6 | Bimaterial | 492 | No HAZ | | | | 293 |
| | Multimat. Discrete HAZ | 492 | 467.2 | 417.4 | 367.9 | 317.8 | 293 |
| | Multimat. Cont. HAZ | 492 | Descending linearly | | | | 293 |
| M=0.42 | Bimaterial | 692 | No HAZ | | | | 293 |
| | Multimat. Discrete HAZ | 692 | 642.1 | 542.3 | 442.5 | 342.7 | 293 |
| | Multimat. Cont. HAZ | 692 | Descending linearly | | | | 293 |

In our previous work [4], the local mechanical behavior was determined spatially on the surface of the flat cross-weld specimens by using digital image correlation integrated tension tests and the experimental results were validated with FE simulations. However, it was found that the agreement between the multi-material discrete HAZ model used in that work and the experimental results was not satisfactory, especially in the HAZ. Therefore, an improved model in which the material properties in HAZ are continuously assigned was required. In multi-material continuous HAZ model (Figure 1(c)), the material properties in the HAZ were successfully assigned continuously by using ABAQUS user-subroutines [12]. The variation of yield strength variation along the length of the specimen is given for multi-material continuous HAZ model in Table 1.

## 3. Results & Discussion

### 3.1. Local stress fields and constitutive behaviour

Stress is uniaxial and uniform during the tensile test of a homogenous specimen until necking. However, triaxial stresses develop during the tensile testing of a cross-weld specimen due to the strength mismatch between different weld zones [13]. Near the interface of two different zones, the deformation of the softer material is prevented

by the stronger material, which results in the generation of triaxial stresses. The triaxiality of stress can be defined by

$$\frac{\sigma_h}{\sigma_{eqv}} = \frac{\frac{1}{3}(\sigma_1+\sigma_2+\sigma_3)}{\frac{1}{\sqrt{2}}\sqrt{(\sigma_1-\sigma_2)^2+(\sigma_2-\sigma_3)^2+(\sigma_3-\sigma_1)^2}} \quad (2)$$

where $\sigma_h$ and $\sigma_i$ (i=1,2,3) denote hydrostatic stress and the principal stresses, respectively. However, due to plane stress assumption "stress biaxiality" is used hereafter to define the state of stress. Note that the stress

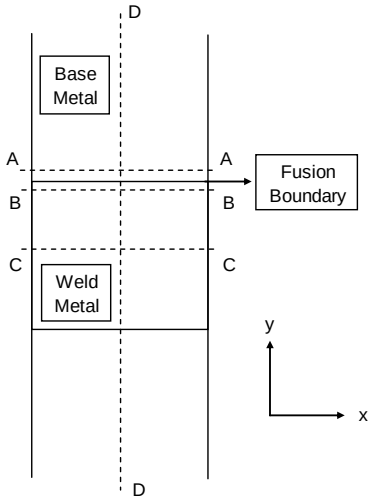


**Figure 2. Schematic view of the cross-weld specimen and locations for local stress evaluation**

biaxiality for a homogeneous specimen deforming under uniaxial loading is 0.33.

The local stress evaluation was carried out on the dashed lines shown in Figure 2. AA line is located in the base metal 0.25mm above the weld/base interface where the effect of the strength mismatch is most dominant due to abrupt transition of the material properties. BB line is located in the weld 0.25mm below the interface. CC line is at the weld centre line. AA, BB and CC lines are along the width of the specimen i.e. in *x*-direction. In order to observe the length of the interface effect in *y*-direction and to obtain the profile of stress biaxiality for bi-material and multi-material models, stress variation along the length of the specimen (line DD) was also obtained.

The variation of stress biaxiality on AA, BB, CC and DD lines obtained from the bi-material and the multi-material models after the specimen is extended 0.85mm from its top end is presented in Figure 3 for both strength mismatch levels. It can be clearly seen that the stress biaxiality arises near the interface and reaches its maximum in the middle of the specimen for all models. Bi-material model exhibits the highest stress biaxialitynear the interface (Figure 3 (a&b)). As the strength mismatch increases it is seen that the stress biaxiality increases. Stress biaxiality is negligible in the centre of the weld (Figure 3 (c)). Because the stress biaxiality is maximum in the middle of the specimen it is worth to determine the variation of the stress biaxiality on DD line (Figure 3 (d)). Note that distance zero corresponds to the weld centre line (WCL). For the bi-material model the strength mismatch at the interface has

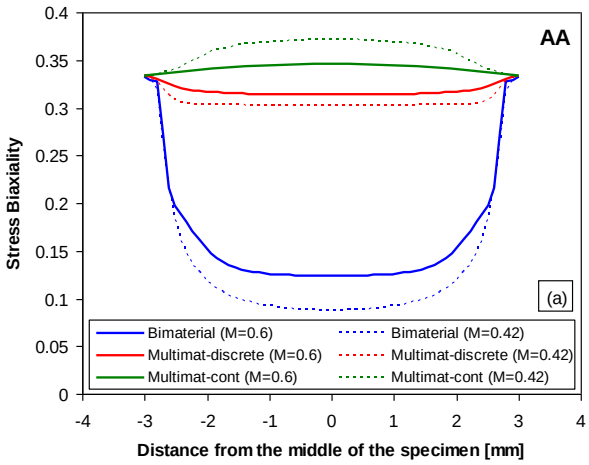


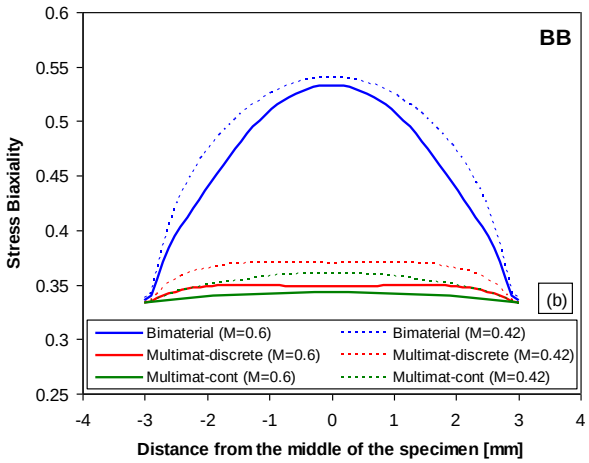


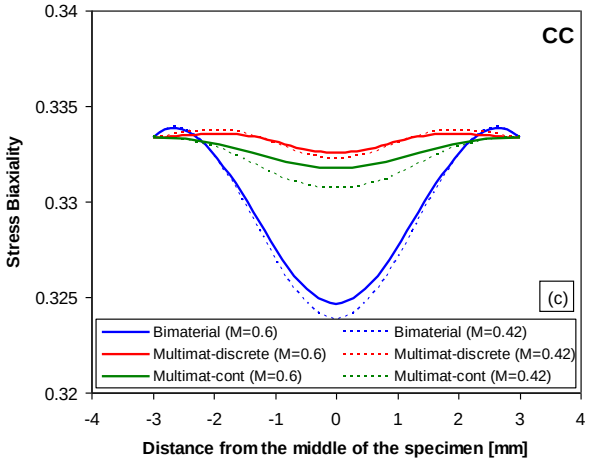

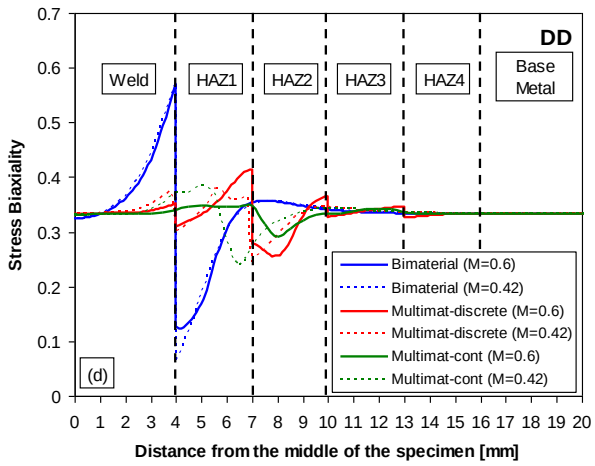


**Figure 3. Stress biaxiality on AA (a), BB (b), CC (c) and DD (d) obtained from bi-material, multi-material discrete HAZ and continuous HAZ models for the strength mismatch levels of M=0.6 and M=0.42 at 0.85mm cross-head displacement**

an influence on the biaxial stress development in a range from WCL to 11mm away from WCL. The stress biaxiality gets larger when approaching to the interface. In the multi-material discrete HAZ model, the stress biaxiality varies in each HAZ layers and getting larger at the interface between each layer. The largest variation is near the interface at 7mm between HAZ1 and HAZ2. Unlike the bi-material and the multi-material discrete HAZ model, the multi-material continuous HAZ model does not exhibit any discontinuity in the profile of stress biaxiality. The largest variation is at 8mm. Note that as the strength mismatch ratio decreases i.e. the base metal gets stronger the bottom curve in the profile move towards the interface.

For the multi-material continuous HAZ model with strength mismatch level of M=0.6, it was observed that the biaxial stress field moves away from the interface along DD line as the deformation proceeds i.e. cross-head displacement increases. It was found that the biaxial stress field at the weld/HAZ interface disappears at 1.36mm cross-head displacement. In the HAZ the biaxial stress field occurring between the currently yielded and un-yielded regions moves towards the base metal and stops at the HAZ/parent interface at 6.8mm cross-head displacement.

In the bi-material and the multi-material discrete HAZ models the deformation in the soft weld metal is constrained by the strong base metal. Tensile stresses develop near the interface in the base metal in the *x*-direction; on the other hand across the interface the weld metal sustains compressive stresses. In multi-material continuous HAZ model the stress development in the *x*-direction is different because there is no abrupt transition of material properties across the interface. However, in continuous HAZ model as the deformation precedes the currently yielding metal will be constrained by the adjacent strain-hardened metal where the yielding had started relatively earlier. Therefore, compressive stresses develop in the *x*-direction in the currently yielding metal whereas tensile stresses accumulate in the adjacent hardened metal.

### 3.2. Global tensile behavior

Global stress-strain behavior of the cross-weld specimens with strength mismatch levels of M=0.6 and M=0.42 obtained from the bi-material and multi-material models and is presented in Figure 4. The global yield point of the cross-weld specimens corresponds to the yield point of the weld metal due to the fact that weld metal starts to yield first since it is softer than the base metal. However, the global hardening behavior is different from the weld metal i.e. the stress required to continue global deformation after yielding is higher compared to the weld metal because the strong base metal is still in the elastic regime and does not plastically deform yet while the weld is yielding.

Global stress-strain curves obtained from the bi-material model for both strength mismatch levels are very similar. Note that the stress at 2.5% strain is still lower than the yield point of both base metals and the material properties abruptly changes at the interface. Therefore, since the base metal does not deform near the interface, the global behavior obtained from the bi-material model for both cross-weld specimens are expected to be the same as long as the base metals are not yielding.

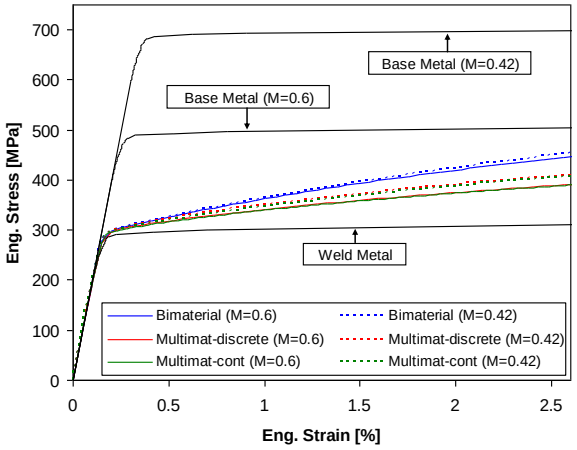


**Figure 4. Global engineering stress-strain curves obtained from bi-material and multi-material models for strength mismatch levels of M=0.6 and M=42 (Engineering stress-strain curves of the weld metal and base metals are also presented)**

On the other hand, the strength mismatch has an influence on the global behavior obtained from the multi-material models. The slope of hardening for M=0.42 is slightly higher than that of M=0.6. Note that multi-material discrete and continuous HAZ models give the same global behavior for the same strength level. In the multi-material models after yielding in the weld the plastic deformation progressively proceeds in the HAZ as long as the global stress reaches the yield point of the HAZ metal near the weld metal.

## 4. Conclusion

Local stress fields develop at the interfaces for all the models studied in this work. The highest biaxial stresses were observed in the bi-material model at the weld/base metal interface. Biaxial stresses also develop at the interface between different HAZ layers in multi-material discrete HAZ model; however, these stresses are not as high as in the bi-material model. In the multi-material continuous HAZ model stress biaxiality occur between the currently yielding region and already hardened region where the plastic deformation had started relatively earlier. Furthermore, the level of stress biaxiality in this model is smaller compared to the other models. Therefore, the multi-material continuous HAZ model is more suited for the study of the local deformation in weld models.

The yield point observed in the global stress-strain curve is determined by the yield point of the soft metal, which is the weld metal for our cross-weld specimens. However, global hardening varies with the contribution of the yielding in the base metal and in the HAZ. It was found that the number of HAZ layers in the discrete HAZ model was sufficient to approximate the continuous HAZ model in terms of global behavior.

## Acknowledgement

The authors would like to thank EDF (formerly British Energy), UK for funding for MOA. Professor Bouchard gratefully acknowledges support from the Royal Society through the Industry Fellowship scheme. MEF is supported by a grant through The Open University from The Lloyd's Register Educational Trust, an independent charity working to achieve advances in transportation, science, engineering and technology education, training and research worldwide for the benefit of all.

## References

[1] *ASME Section I, ASME Boiler and Pressure Vessel Code, Section I: Rules for Construction of Power Boilers*. 2010, ASME: New York, USA, .

[2] Spindler, M., *Effects of plastic strain and heat treatment on microstructure and properties of 316 stainless steel tubing (Personal communication)*. 2008.

[3] Spindler, M., *Post-weld heat treatment of austenitic stainless steel welds in boiler units (Personal communication)*. 2011.

[4] M. Acar, S.G., P. J. Bouchard and M. E. Fitzpatrick, *Effect of Prior Cold-work on the Mechanical Properties of Weldments*, in *Society of Experimental Mechanics (SEM) Annual Conference* 2010, Society of Experimental Mechanics (SEM) Annual Conference Proceeding: Indianapolis USA. p. 283.

[5] Turski, M., et al., *Spatially Resolved Materials Property Data From a Uniaxial Cross-Weld Tensile Test.* Journal of Pressure Vessel Technology, 2009. **131**(6): p. 061406-7.

[6] Kou, S., *Welding Metallurgy*. 2 ed. 2003: Wiley-Blackwell.

[7] Genevois, C., A. Deschamps, and P. Vacher, *Comparative study on local and global mechanical properties of 2024 T351, 2024 T6 and 5251 O friction stir welds.* Materials Science and Engineering: A, 2006. **415**(1-2): p. 162-170.

[8] Lockwood, W.D., B. Tomaz, and A.P. Reynolds, *Mechanical response of friction stir welded AA2024: experiment and modeling.* Materials Science and Engineering A, 2002. **323**(1-2): p. 348-353.

[9] Lockwood, W.D. and A.P. Reynolds, *Simulation of the global response of a friction stir weld using local constitutive behavior.* Materials Science and Engineering A, 2003. **339**(1-2): p. 35-42.

[10] Rodrigues, D.M., et al., *Numerical study of the plastic behaviour in tension of welds in high strength steels.* International Journal of Plasticity, 2004. **20**(1): p. 1-18.

[11] Liu, S. and Y.J. Chao, *Determination of global mechanical response of friction stir welded plates using local constitutive properties.* Modelling and Simulation in Materials Science and Engineering, 2005. **13**(1): p. 1.

[12] *ABAQUS Standard/User's Manual, Version 6.7*. 2007, Dassault Systemes

[13] Kim, Y.-J. and C.-S. Oh, *Finite element limit analyses of under-matched tensile specimens.* Engineering Fracture Mechanics, 2006. **73**(10): p. 1362-1378.